Two-color transient pumping in Ni-like silver at 13.9 and 16.1 nm

Jaroslav Kuba,* Annie Klisnick, David Ros, Paul Fourcade, and Gérard Jamelot
Laboratoire de Spectroscopie Atomique et Ionique, Université Paris–Sud, Bâtiment 350, 91405 Orsay Cedex, France

Jean-Luc Miquel and Nathalie Blanchot
CEA Limeil-Valenton, 94195 Villeneuve Saint-Georges Cedex, France

Jean-François Wyart
Laboratoire Aimé Cotton, Université Paris–Sud, Bâtiment 505, 91405 Orsay, France
(Received 17 February 2000; published 13 September 2000)

We report on progress in the optimization and understanding of the collisional pumping of x-ray lasers in the transient regime using an ultrashort subpicosecond heating pulse. An irradiation scheme using a frequency-doubled 600-ps laser pulse to preform the plasma is tested. The effect of traveling-wave irradiation on the time-integrated and time-resolved lasing signal at the $4d\ ^1S_0 \rightarrow 4p\ ^1P_1$ Ni-like Ag line is studied in detail. Under specific irradiation conditions, strong lasing is also obtained on another spectral line at 16.05 nm that is identified as the $4f\ ^1P_1 \rightarrow 4d\ ^1P_1$ transition in Ni-like Ag.

PACS number(s): 42.55.Vc, 52.50.Jm, 42.60.By, 32.30.Rj

I. INTRODUCTION

Since the first demonstration in 1985 [1], significant progress has been made in improving the efficiency of x-ray lasers (XRL's). One of the main goals being currently pursued by researchers is the production of a so-called ''table-top'' XRL that would use a small-scale laser as a driver.

''Standard'' collisional XRL's pumped by a relatively long laser pulse (duration of 100–600 ps) now routinely reach a saturated gain-length product of 15, with a pump energy of typically 100–1000 J [2]. These XRL's also rely on the use of a low-energy prepulse preceding the main pulse by a few ns [3]. The Ne-like zinc XRL emitted at 21.2 nm and operated in a half-cavity was successfully used at Laboratoire de Spectroscopie Atomique et Ionique, France as a coherent x-ray source for interferometry applications [4].

The pump energy requirement was dramatically reduced to several J recently, when the development of chirped pulse amplification (CPA) laser technology enabled the testing of the transient collisional excitation (TCE) pumping scheme. This scheme was proposed as early as in 1989 [5], and investigated theoretically by several authors [6–8]. The first experimental demonstration of transient gain was achieved in 1995 in Ne-like Ti [9], and a saturationlike regime was first reported in the same element in 1998 [10].

The transient pumping scheme consists of two-stage target irradiation by two consecutive laser pulses. The initial long-duration and low-intensity pulse creates a plasma containing a large population of the desired ion species (i.e., nickel-like, neonlike, or possibly others). The second subpicosecond-duration, high-intensity laser pulse heats the preformed plasma and—due to the collisional electron-ion excitation—creates a *transient* inversion of population. Since the population inversion is nonstationary, and short lived (a few ps), compared with the transit time of the amplified photons along the active plasma (~30 ps for a 1-cm target), the ultrashort pulse must heat a local region which travels at the velocity of light in the direction of x-ray amplification. This is achieved by tilting the wave front of the short pulse energy, leading to a traveling wave (TW) irradiation geometry. The beneficial effect of implementing TW irradiation in pumping a laser was studied theoretically in Ref. [11] in the context of dye lasers. One of the possible methods to generate a TW irradiation consists in tilting slightly one of the compressor gratings [12].

Using a TW, an increase in the XRL intensity of a factor of ~300—in comparison with the TCE without the TW—was reported recently [13] for a 500-fs pumping pulse. A time-integrated gain coefficient of 14.5 cm^{-1} was measured at the Ni-like $J=0-1$ $4d$-$4p$ silver line at 13.9 nm. A roll-off from the exponential intensity versus length increase—similar to what is observed at saturation—was observed for plasma lengths above 7 mm. However, refraction was noted to be an important factor in such experiments with short-pulse pumping. The deflection angle of the x-ray laser beam was found to be as high as 13 mrad after traveling in a 1-cm-long plasma. Similar experiment with Ni-like Ag was also performed at CEA with analogous results [14]. However, in previous experiments using 130-ps pumping pulses [13], the deflection angle of the laser output at 13.9 nm was only 3 mrad, although emitted from a longer, 2-cm plasma.

With the aim of improving the propagation of the amplified photons, we carried out an experiment that is reported in this paper. In this experiment the long pulse that preforms the plasma was frequency doubled, while the ultrashort heating pulse was left at the fundamental laser frequency ($\lambda = 1.057\ \mu m$). In this case the 1ω heating pulse is absorbed at—and slightly above—the critical density $N_c(1\omega)$ which is four times smaller than the critical density $N_c(2\omega)$ for the 2ω pulse. This means that the ultrashort pulse is absorbed in a region which is coronal for the 2ω preformed plasma. The

*Also at Faculty of Nuclear Sciences and Physical Engineering, Czech Technical University in Prague, Břehová 7, 115 19 Prague 1, Czech Republic.

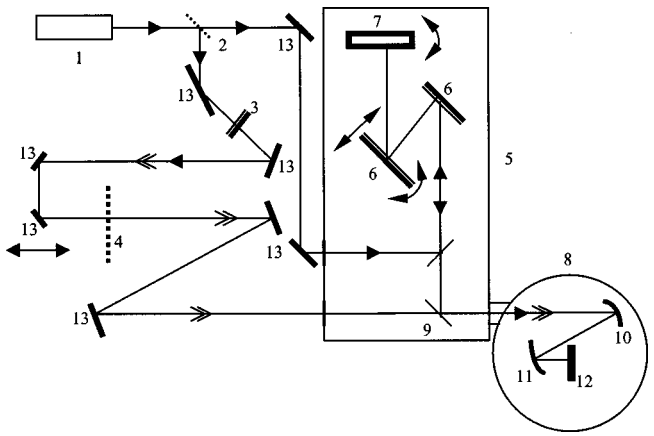

FIG. 1. Experimental setup showing the optical paths for the short and long laser pulses: (1) P102 laser, (2) polarizer, (3) KDP crystal, (4) 1ω filter, (5) vacuum compressor, (6) compressor gratings, (7) hollow roof prism, (8) target chamber, (9) dichroic mirror, (10) cylindrical mirror, (11) parabolic mirror, (12) target, and (13) mirrors.

expected advantages over a $1\omega/1\omega$ configuration are twofold: (i) the heated zone is located further from the target surface, in a region where the density gradients are smoother; and (ii) the heating pulse is absorbed in the coronal, high-temperature region where the ionization stage is higher than it would be at the critical density of the preformed plasma. Thus the main part of the energy of the ultrashort pulse is used to heat the electrons, and thereby promote a population inversion on the lasing line of interest. Finally, as we report in Sec. V, this configuration provided conditions suitable to generate strong lasing on a previously unobserved lasing line at 16.05 nm, which sometimes surpassed the 13.9-nm line. Following semiempirical calculations, we identify this line to be the $4f\ ^1P_1 \rightarrow 4d\ ^1P_1$ transition in Ni-like silver.

II. EXPERIMENTAL ARRANGEMENT

The experiment was conducted at the P102 laser facility in CEA Limeil—Valenton, France. The P102 laser is a hybrid CPA system consisting of a Ti:sapphire front end and a mixed Nd:glass power chain [15]. A part of the beam is compressed in a vacuum grating compressor to a 350-fs minimal duration, and the other part is reamplified in the last amplifier stage. The plasma was created by irradiating flat silver slabs of 1.50–11.80 mm in length, with two successive laser pulses: a long 600-ps pulse (the preforming pulse), followed by a compressed 400-fs pulse (the heating pulse). Both pulses originate from the same stretched and amplified laser pulse (Fig. 1). The maximum energy available was 70 J in the long pulse and 30 J in the short pulse.

Each laser beam is focused down to a line $\sim$1.9 cm long by a combination of a cylindrical mirror and of an off-axis parabola. The line foci thus generated are superimposed with a precision better than 20% of the focus linewidth. The focal line is longer than the target length to avoid creation of cold plasma at the target ends.

The focusing system used introduces an intrinsic fast TW running along the target at a velocity of $v \sim 6.5c$, where c is the speed of light. To generate a TW at the appropriate velocity of c we used the technique initially validated in Refs. [12] and [13]. This technique consists in tilting slightly the second grating of the compressor to induce a tilt of the wave front of the compressed, ultrashort pulse. By adjusting the tilt angle we were able to control the speed and the direction of the traveling wave. We could also exactly compensate for the intrinsic TW given by the focusing optics in order to irradiate the target with no TW at all.

The beam carrying the long preforming pulse was frequency doubled by a well-known doubling crystal KDP with a $\sim$43% efficiency. In the first period of the experiment we varied several parameters in order to find the conditions that optimized the 13.9-nm laser emission. These optimum conditions were a focal width of 70 μm, and energies of $\sim$3 J/cm (at 2ω) in the 600-ps preforming pulse and of $\sim$7.5 J/cm in the 450-fs heating pulse, with a temporal separation of 250 ± 50 ps between both pulses. Unless otherwise specified the results presented below were obtained with these conditions.

The XRL output was recorded at both ends of the target. In one direction a transmission grating spectrometer (TGS) ''SPARTUVIX'' [16] provided the time-integrated spectrum, with angular resolution in the vertical plane and integration in the horizontal plane over a 3–8-mrad interval (according to the adjustment). In the opposing direction a flat-field grating spectrometer (FFS) [17] recorded the time-integrated spectrum with angular resolution in the horizontal plane, and integration in the vertical plane over a $\sim$2-mrad interval. The FFS was thus able to provide information about the refraction of the x-ray laser beam in the horizontal plane. This information was used to set the TGS at the angular peak of emission. For some shots the TGS was equipped with a soft x-ray streak camera instead of a thinned, back-illuminated charge-coupled device (CCD), to provide temporal history of the laser emission with a $\sim$5-ps resolution.

III. CONTROLLING THE X-RAY LASER OUTPUT WITH THE TRAVELING WAVE

The influence of the traveling wave on the XRL intensity was studied in both directions with the two spectrometers. The TW velocity toward the TGS was set at $v = c$, while due to technical reasons the velocity in the other direction was at $v \sim 1.085c$. However, this difference is not expected to play a significant role.

We examined a triplet of shots at nearly same long and short pulse energies with the following TW conditions: (a) the TW towards the FFS ($v \approx -c$), (b) without a TW (i.e., $v \rightarrow \infty$), and (c) the TW toward the TGS ($v = c$). The spectra obtained in the three cases on the TGS are shown in Fig. 2. The vertical direction in the images displays the dependence of the spectral intensity versus the vertical angle. One can see that the intensity of $4d$-$4p$ line at 13.9 nm increases dramatically when the traveling wave is directed toward the spectrometer [Fig. 2(c)], causing a strong saturation of the detector. The satellite peaks appearing on both sides of the 13.9-nm line in Fig. 2(c) are due to the diffraction of this radiation on the periodic grid supporting the transmission

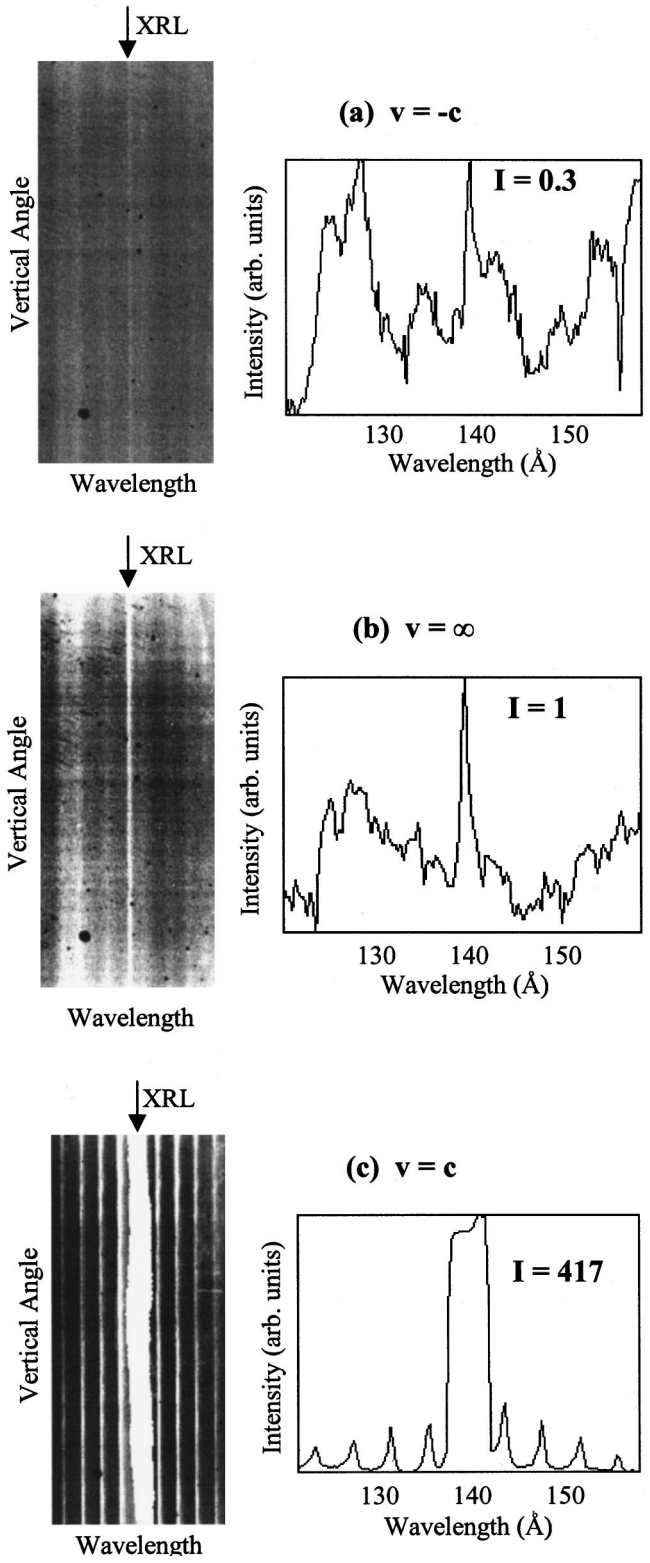

FIG. 2. Demonstration of the traveling-wave effect on the $4d$-$4p$ output intensity at the TGS spectrometer. (a) The TW is directed backward. (b) Without a TW. (c) The TW is directed forward with respect to the spectrometer. The $4d$-$4p$ line is strongly increased in case (c), where it saturates the detector. The secondary peaks around arise from diffraction onto the grid supporting the grating.

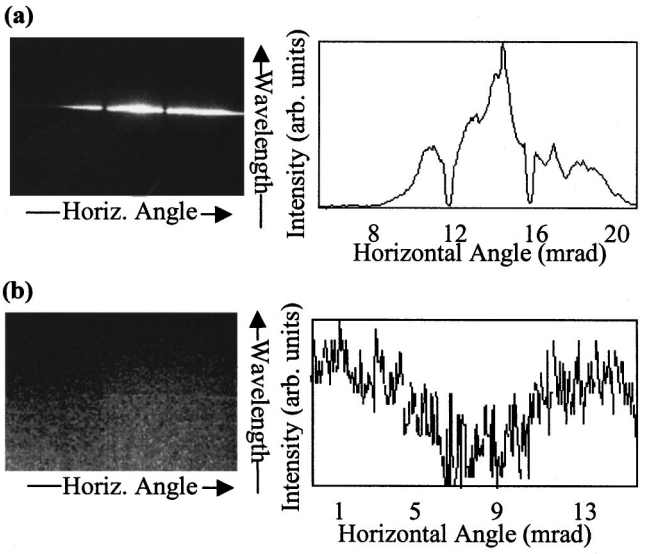

FIG. 3. For the same shots as in Fig. 2, two of the three spectra showing the $4d$-$4p$ line in the other direction, obtained by the FFS spectrometer: (a) The TW is directed toward the FFS spectrometer. (b) Without a TW. The image corresponding to case (c) showed no lasing line.

grating. Since the ratios between the intensities of the successive diffraction peaks are known, we were able to retrieve the value of the intensity of the central peak, even when saturating the detector.

Spectra were obtained for the same three shots in the other direction by the FFS. Figure 3 displays those, which correspond to Figs. 2(a) and 2(b), respectively. Here the horizontal direction in the images gives the dependence of the spectral intensity versus horizontal angle, with respect to fiducial wires, which give the vertical dark lines in the spectra. The 13.9-nm line was not visible above background in case (c), when the TW is directed backward with respect to the spectrometer; hence the image is not shown. The 13.9-nm line is very weak in Fig. 3(b) (no TW), and only an estimate of the measured peak intensity can be made. As above, directing the TW toward the spectrometer leads to a strong enhancement of the lasing emission [Fig. 3(a)].

Table I summarizes the relative intensities (i.e., normalized to the ''no-TW'' case) measured in both spectrometers for cases (a), (b), and (c). It can be seen that both spectrometers indicate that the TW enhances the x-ray laser output by a large factor of ~300–400, compared to the case where the TW is not present. This large enhancement indicates that the

TABLE I. Peak intensity values (in arbitrary units) measured at 13.9 nm with each of the spectrometers when varying the direction of the TW irradiation [cases (a) and (c)] or canceling the TW [$v=\infty$—case (b)]. The asterisk means a value is not measurable.

	(a) $v=-c$	(b) $v=\infty$	(c) $v=c$
TGS	0.3	1	~417
FFS	~300	1	*

transient high gain has a short duration. The lasing line intensity is further reduced by a smaller factor of ~0.3 when the TW is directed away from the plane of observation. Such a strong enhancement is a result of the short duration used for the heating pulse. With a longer pulse (1.7 ps) the effect of the TW in our previous work [13] was reduced to a 80× enhancement.

The effect of the TW on the temporal history of the x-ray laser signal was investigated by coupling a streak camera with a resolution of ~5 ps at the output of the TGS spectrometer. Figure 4 compares the variation of the 13.9-nm intensity, integrated over the linewidth, in the case with a TW [Fig. 4(a)] and without a TW [Fig. 4(b)]. The target length was of 9.8 mm for these two shots. One can see that the duration of the XRL pulses is very short both with and without TW.

In both Figs. 4(a) and 4(b) the XRL pulse exhibits a near-symmetric shape. However, the temporal resolution of $T_R = 5$ ps which is comparable with the duration of the lasing signal does not allow one to detect a possible asymmetry between the rising and falling edges of the pulse. Due to the saturation of the detector at the 13.9-nm central peak, the temporal trace shown in Fig. 4(a) was taken from the closest satellite peak produced by diffraction on the supporting grid (see above). The duration of the XRL pulse was found to vary from shot to shot. However it was noted that on average the duration was shorter when the TW was applied. The average full width at half maximum (FWHM) measured was 17.3 ps without a TW and 8.7 ps with a TW. These values were obtained after deconvolution from the instrumental resolution, using the formula $\tau' = \sqrt{\tau^2 - T_R^2}$, where T_R is the temporal resolution of the detector, τ stands for the measured duration of the signal, and τ' is the actual duration taking into account the detector resolution.

Such a shortening of the pulse duration can be understood from simple considerations on photon propagation in the high gain active zone. In the case without a TW, the gain coefficient is—at a given time—the same along the whole plasma column (i.e., it does not depend on the spatial coordinate along the target, but it depends on time). In the limit case where the duration of the gain is extremely short compared to the photon transit time along the plasma column, the output XRL pulse results from the integrated contribution of spontaneous photons statistically created along the whole length and amplified at a short distance. The overall duration in this case reflects the photon transit time (i.e., 33 ps for a 1-cm plasma). Conversely, when a TW traveling at $v = c$ is applied, the main contribution to the output XRL signal comes from photons created at one end of the plasma column and amplified over the entire length (due to the high gain that is applied at each point of the active zone). The pulse duration in this case corresponds directly to the gain duration; hence it is shorter than in the case without a TW.

This can be shown from a simple small-signal model, which calculates the intensity resulting from amplified spontaneous emission (ASE) in a plasma column. The gain coefficient G is assumed to be constant and equal to 30 cm^{-1} during the time interval $\Delta t = 9$ ps, and equal to zero outside this period. The plasma column is 1 cm in length. The calculated temporal histories of the intensity in the case with and without a TW are displayed in Fig. 5. The duration of the XRL intensity pulse with a TW corresponds exactly to the duration of the gain maximum (9 ps), while the duration of the XRL without a TW is comparable (although slightly shorter) to the photon transit time, and hence is significantly longer than in the previous case.

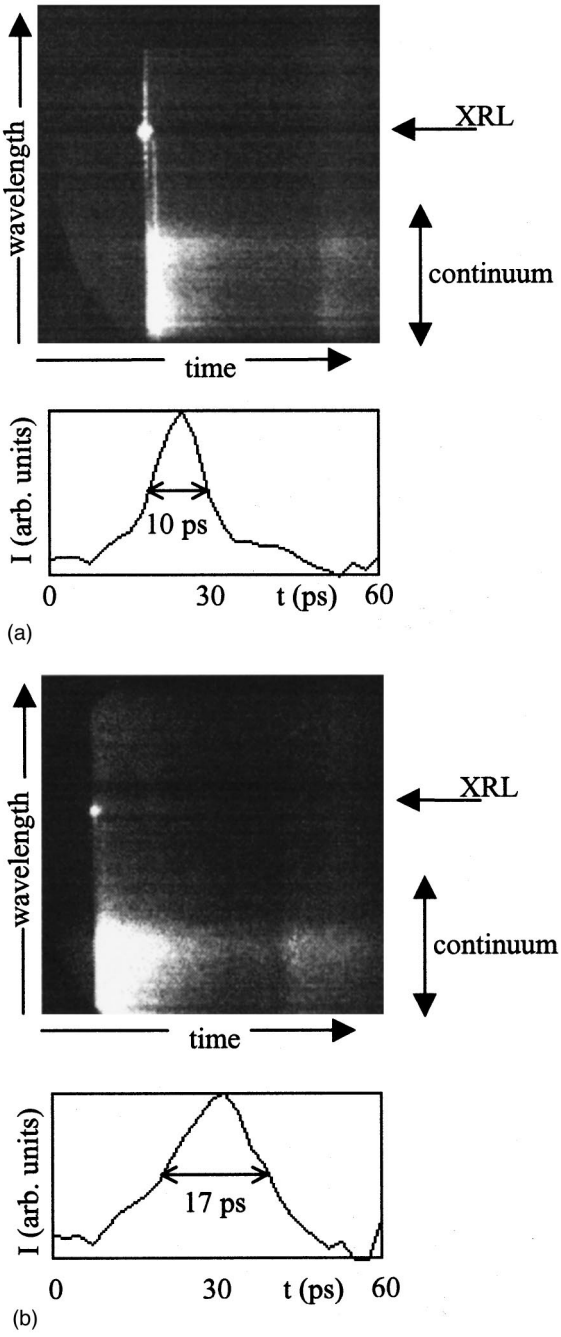

FIG. 4. Difference in time profile of the XRL output intensity between the case with and without a TW. (a) CCD camera image with TW and temporal profile at the XRL wavelength (FWHM duration of 10 ps). (b) CCD camera image without a TW and the same temporal profile (FWHM duration of 17 ps). Both figures show the data before deconvolution due to the resolution of the streak camera.

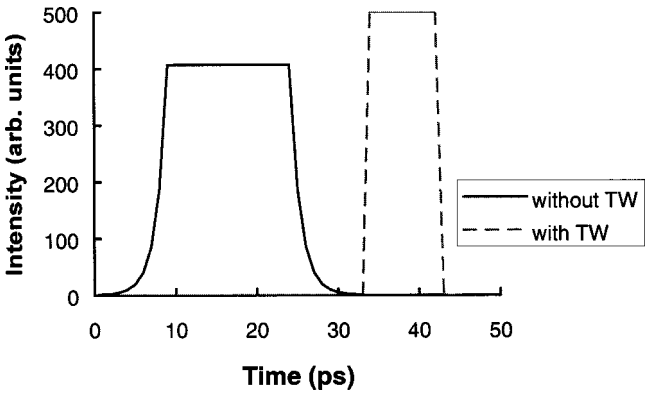

FIG. 5. Temporal history of the XRL intensity calculated from a simple model (a) without a TW and (b) with a TW. Note that the vertical scales in both cases are not comparable. The model qualitatively reproduces the shorter duration observed in the case with a TW.

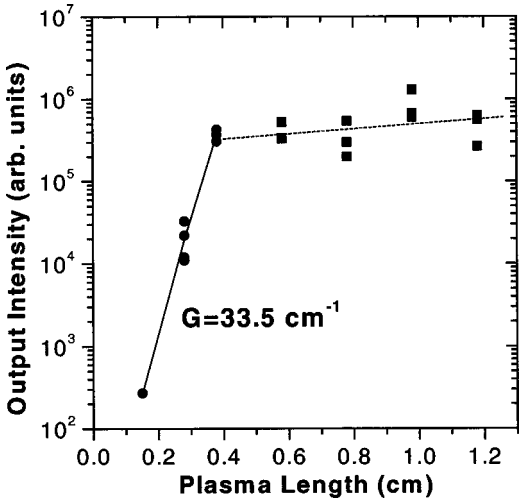

FIG. 6. Plot of the XRL output intensity vs the target length. A small signal gain of 33.5 cm^{-1} is inferred for target lengths shorter than 3.8 mm.

IV. CHARACTERISTICS OF THE 13.9-nm EMISSION

The angular profile of the 13.9-nm lasing emission in the horizontal plane was investigated with the FFS spectrometer (when the TW was directed toward it). We observed that the profile was often asymmetric around the peak intensity, with a broader falling edge at larger output angles. The FWHM divergence and deflection angle of the XRL beamlet were studied statistically for all available shots. The measured divergence values were found to be distributed symmetrically around a maximum at 3 mrad, with a FWHM distribution of 2 mrad. This is significantly smaller than the divergence of more than 6 mrad observed in the 1ω-1ω experiment previously carried out at Laboratoire pour l'Utilisation de Lasers Intenses, France (LULI) [13]. The 2ω-1ω irradiation scheme used here was actually noted to yield the smallest divergence compared to the other irradiation schemes tested during the experimental campaign at P102 [18]: 1ω-1ω, 1ω-2ω.

For most of the shots performed in the standard conditions with a TW, the deflection angle of the 13.9-nm beamlet was in the 10–12-mrad range. This is slightly smaller than the 13-mrad angle observed in the LULI experiment. Larger values (14 mrad or more) were obtained when the TW was switched off, and when the delay between the preforming pulse and the ultrashort pulse was set to 800 ps instead of 250 ps.

When varying the energy of the 600-ps pulse in the range 1.6–3.2 J/cm, no clear influence on the 13.9-nm intensity could be found. On the other hand, the 13.9-nm intensity increased exponentially when the energy of the 400-fs pulse was enhanced from 5.8 to 8.4 J/cm. These results can be interpreted as the intensity of the lasing emission being closely linked to the peak electron temperature at the time of plasma heating by the 400-fs pulse, through the rate of collisional excitation pumping. The higher the energy of the short pulse—within the limits investigated here—the higher the peak temperature, and hence the stronger the XUV amplification.

The gain coefficient at 13.9 nm was measured with the TGS spectrometer by varying the plasma length between 1.5 and 11.8 mm. The plot of intensity versus length is displayed in Fig. 6. An exponential increase corresponding to a gain coefficient (derived from the Linford formula) of 33.5 cm^{-1} is observed for plasma lengths up to 3.8 mm (i.e., a gain-length product of 12.7), which then abruptly turns to a linear increase for larger lengths. This saturationlike behavior was already observed at LULI, and is also reported in other transient pumping experiments [19]. However, in the LULI experiments the gain coefficient was only 15 cm^{-1}, and the intensity roll-off was observed for plasma lengths above 7 mm (a gain-length product of 10.5). It is notable that a theoretical estimate of the saturation gain length as well as experiments performed with the ''standard'' quasi-steady-state pumping (i.e., with 100-ps pump pulses) produce larger values, of the order of 16. This difference is likely due to the combined effects of saturation and refraction, which lead to the lower effective amplification.

V. STRONG LASING LINE AT 16.05 nm

Strong lasing was also observed on a longer wavelength line measured at 16.05 ± 0.05 nm. The intensity of this line sometimes exceeded the 13.9-nm line. Figure 7 displays a time-integrated spectrum in which the 16.05-nm line, and the $4d$-$4p$ line exhibits a similar intensity. Both lines give rise to a fringe pattern due to the diffraction onto the grid supporting the transmission grating. Those satellite peaks actually gave the opportunity to infer the wavelength of the new lasing line from the well-known wavelength of the $4d$-$4p$ line. The identification of the 16.05-nm line to the $4f\ ^1P_1 \rightarrow 4d\ ^1P_1$ transition in Ni-like silver was made following recent semiempirical calculations of energy levels in this ion, performed at Laboratoire Aimé Cotton, France. These calculations use the Slater-Condon parametric method with generalized least-square fits [20]. By including several new available experimental wavelengths, the new calculations gave refined predictions over the formerly published ones [20]. The wavelength of the $4f\ ^1P_1 \rightarrow 4d\ ^1P_1$ line is predicted to be 15.97 ± 0.1 nm. Recent calculations performed at

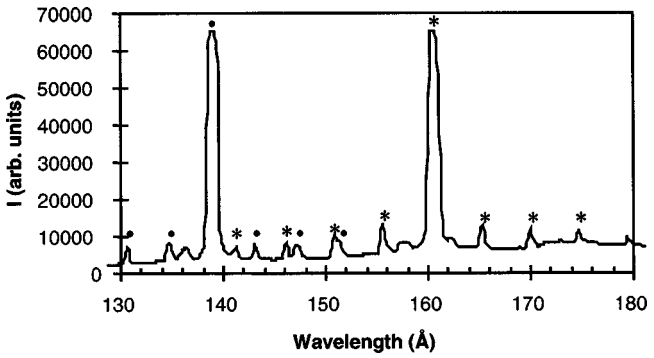

FIG. 7. Time-integrated spectrum showing the 13.9-nm line and a strong new line located at 16.05 nm. Both lines give rise to a fringe pattern by diffraction of radiation on the grid supporting the transmission grating. These satellite peaks (• and *) are used to infer the peak intensity of the lines when the central peak saturates the detector. The plasma length is 6 mm; the TW at $v=c$ is toward the spectrometer.

Lawrence Livermore National Laboratory (LLNL) also confirm this identification [21].

The observation of the $4f$-$4d$ line with a weak intensity was reported in Ni-like Zr and Mo by the LLNL group [19,22], and interpreted as pumped in part by self-photopumping from the strong $3d$-$4f$ resonance line [23]. Here our observation shows, for the first time to our knowledge, that lasing as strong as on the $4d$-$4p$ line can be obtained on the $4f$-$4d$ line, although the relative contributions of photopumping and collisional pumping in the $4f$-$4d$ amplification still needs to be experimentally investigated. The intensity of the 16.05-nm line was very unstable from shot to shot, and showed a very high sensitivity to the energy of the short pulse. For this reason no reliable measurement of the gain coefficient could be made. The intensity data plotted in Fig. 8 show that there could exist some correlation of the intensity of the $4f$-$4d$ line with respect to the $4d$-$4p$ one. Even though the functional dependency is not clear, one can see that—except for one data point—the intensity of the $4f$-$4d$ line rises considerably with the $4d$-$4p$ line intensity.

Finally, this new line was observed only under specific conditions of irradiation, namely (i) when the TW was directed toward the spectrometer, (ii) when the temporal delay between the long and ultrashort pulses was set to 250 ps, (iii) for the 2ω-1ω irradiation scheme only, and (iv) for target lengths greater than 3.8 mm (at this length the $4d$-$4p$ line was already saturated). The $4f$-$4d$ line never appeared for the other configurations tested (1ω-2ω; 1ω-1ω; see Ref. [18]). These indications may help numerical simulations to understand better the conditions and mechanisms involved in lasing on the $4f\ ^1P_1 \rightarrow 4d\ ^1P_1$ line.

VI. CONCLUSIONS

With the aim of improving the propagation of x-ray lasers pumped in the transient regime, we tested a two-color irradiation scheme in which the preforming pulse is at a shorter wavelength than the ultrashort heating pulse. A large gain of 33.5 cm^{-1} is obtained on the Ni-like Ag $4d\ ^1S_0 \rightarrow 4p\ ^1P_1$ line at 13.9 nm with modest energy requirements on the target of 3 and 7.5 J/cm for long and short pulses, respectively. The divergence of the x-ray laser beamlet is substantially improved over the previous experiment performed at LULI with a 1ω irradiation (3 mrad instead of 6 mrad). The deflection angle is still large ($\sim$10 mrad). This indicates that refraction affects strongly the propagation of the amplified photons. However, saturation is believed to play a role in the roll-off of the intensity versus plasma length observed for $L>4$ mm.

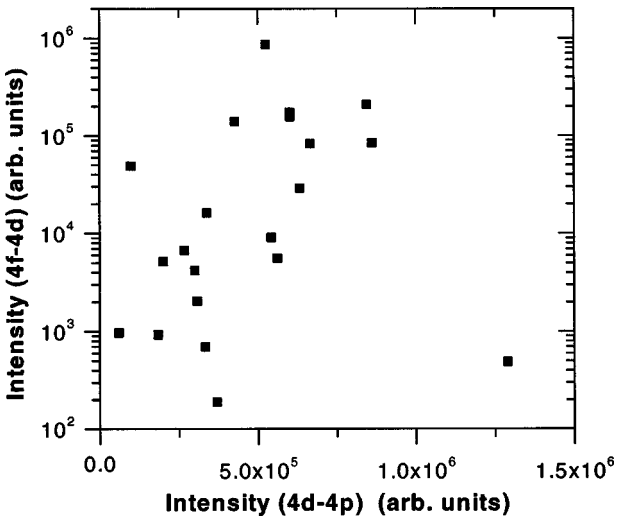

FIG. 8. Plot of experimental data showing that there seems to exist a correlation between the intensities of the $4d\ ^1S_0 \rightarrow 4p\ ^1P_1$ and $4f\ ^1P_1 \rightarrow 4d\ ^1P_1$ laser lines. Note that the horizontal scale ($4d$-$4p$) is linear, while the vertical one ($4f$-$4d$) is logarithmic.

The effect of traveling-wave irradiation on the output lasing signal at 13.9 nm was investigated in detail. A $(300-400)\times$ enhancement factor was observed when a TW running at $v=c$ was applied to the 400-fs heating pulse. This enhancement could be observed in the two opposite directions by controlling the direction of the TW. A shortening of the duration of the x-ray laser pulse from $\sim$17 to $\sim$9 ps was noted on the time-resolved spectra when a TW was applied.

Finally, a new lasing line at 16.05 nm was observed under specific irradiation conditions with intensity, which sometimes surpassed the 13.9-nm line. Following semiempirical calculations we identify this line to the $4f\ ^1P_1 \rightarrow 4d\ ^1P_1$ transition in Ni-like silver. The understanding of the plasma conditions that favor strong lasing on this line and of the potential role of photopumping requires further investigation.

ACKNOWLEDGMENTS

The authors wish to thank I. Legoff, A. Pierre, A.-M. Couvret, and G. Lidove (CEA-Limeil) for their technical assistance in the experiment. Calculations relevant to the implementation of the TW were kindly provided by J.-C. Chanteloup (LULI). The authors also wish to acknowledge the support of and fruitful discussions with S. Jacquemot (CEA-Bruyères le Chatel). This work was conducted in the frame of the TMR X-ray Laser Network under Contract No. ERBFMRXCT98-0185.

[1] D. L. Matthews *et al.*, Phys. Rev. Lett. **54**, 110 (1985); S. Suckewer *et al.*, *ibid.* **55**, 1753 (1985).
[2] A current state of the art of the field can be found in *X-Ray Lasers 1998*, edited by Y. Kato, H. Takuma, and H. Daido, IOP Conf. Proc. No. 159 (Institute of Physics and Physical Society, Bristol, 1999).
[3] B. Rus, A. Carillon, P. Dhez, P. Jaeglé, G. Jamelot, A. Klisnick, M. Nantel, and Ph. Zeitoun, Phys. Rev. A **55**, 3858 (1997); T. Boehly *et al.*, *ibid.* **42**, 6962 (1990); J. Nilsen *et al.*, *ibid.* **48**, 4682 (1993); E. E. Fill *et al.*, Proc. SPIE **2520**, 134 (1995).
[4] Ph. Zeitoun *et al.*, in *X-Ray Lasers 1998* (Ref. [2]), p. 669; F. Albert, *ibid.*, p. 673.
[5] Y. V. Afanasiev and V. N. Shlyaptsev, Kvant. Elektron (Moscow) **16**, 2499 (1989) [Sov. J. Quantum Electron. **19**, 1606 (1989)].
[6] S. Maxon *et al.*, Phys. Rev. Lett. **70**, 2285 (1993).
[7] K. G. Whitney, A. Dasgupta, and P. E. Pulsifer, Phys. Rev. E **50**, 468 (1994).
[8] S. B. Healy, K. A. Janulewicz, J. A. Plowes, and G. J. Pert, Opt. Commun. **132**, 442 (1996).
[9] P. V. Nickles *et al.*, Phys. Rev. Lett. **78**, 2748 (1997).
[10] M. P. Kalachnikov *et al.*, Phys. Rev. A **57**, 4778 (1998).
[11] J. Klebniczki, Zs. Bor, and G. Szabó, Appl. Phys. B: Photophys. Laser Chem. **46**, 151 (1988).
[12] J.-C. Chanteloup *et al.*, J. Opt. Soc. Am. B **17**, 151 (2000).
[13] A. Klisnick *et al.*, in *X-ray Lasers 1998* (Ref. [2]), p. 107; J. Opt. Soc. Am. B **17**, 1093 (2000).
[14] S. Jacquemot, L. Bonnet, J. L. Miquel, and S. Hulin, in *X-Ray Lasers 1998* (Ref. [2]), p. 363.
[15] N. Blanchot, C. Rouyer, C. Sauteret, and A. Migus, Opt. Lett. **20**, 395 (1995); C. Rouyer *et al.*, J. Opt. Soc. Am. B **13**, 55 (1996).
[16] J.-L. Bourgade *et al.*, Rev. Sci. Instrum. **59**, 1840 (1988).
[17] A. Klisnick, G. Jamelot, J. C. Lagron, and L. Vanbostal, LULI Annual Report, p. 179 (1996) (in French).
[18] J. L. Miquel *et al.*, Proc. SPIE **3776**, 24 (1999).
[19] J. Dunn *et al.*, in *X-Ray Lasers 1998* (Ref. [2]), p. 51.
[20] J. F. Wyart, Phys. Scr. **36**, 234 (1987).
[21] J. Nilsen *et al.*, in *X-Ray Lasers 1998* (Ref. [2]), p. 135.
[22] Y. Li *et al.*, Phys. Rev. A **58**, R2668 (1998).
[23] J. Nilsen, J. Opt. Soc. Am. B **14**, 1511 (1997).